On the Catalytic Effect of Ethers during Hydroboration of Alkenes

Daniel J. S. Sandbeck and Allan L. L. East*

Department of Chemistry and Biochemistry, University of Regina, 3737 Wascana Parkway, Regina, SK, S4S 0A2, Canada

*allan.east@uregina.ca

ABSTRACT

Coupled-cluster and density-functional computations are used to test Brown's hypothesis for the catalytic effect of ether solvents upon hydroboration of alkenes. Two diboranes are tested: B_2H_6 and Brown's dimer (9-BBN)$_2$ (9-BBN ≡ 9-borabicyclo[3.3.1]nonane, $C_8H_{15}B$). Comparisons to Brown's data are made for (i) infrared and ^{11}B-NMR spectral features, and (ii) an equilibrium constant for adduct formation. Transition-state searches were performed for four S_N2-type reaction steps, exploring a hypothesis published by Schleyer long ago. We concur with Brown regarding the value for the equilibrium constant for adduct formation, and explain why this should not be computed with traditional gas-phase ΔG estimates from computational chemistry codes. All 4 S_N2-type transition states were located for B_2H_6 + tetrahydrofuran, but not all are expected to exist for the 9-BBN dimer due to steric hindrance for S_N2 approach.

1. INTRODUCTION

Hydroboration is the addition of a borane B-H bond across an unsaturated multiple bond, generally of an alkene. Boranes BR_2H generally appear as H-bridged dimers, $(BR_2H)_2$; their dissociation equilibria lie heavily to the left. Nobel prizewinner H.C. Brown[1] proposed in 1982 a mechanism for hydroboration that nicely explained many aspects, including the catalytic effect of ethers. Most computational studies (e.g. Schleyer,[2] Houk,[3] and now Ess[4] and Singleton[5]) have focused on the last step in the mechanism, because this affects the product distributions. This project focuses instead on the complete mechanism, which appears not to have been confirmed by modern computational means. The purpose of this study was to use quantum chemistry computations to test Brown's mechanism of hydroboration of alkenes, including his explanation of the catalytic effect of tetrahydrofuran solvation.

Brown's mechanism in ether solvent was steps 3-5 of the following six reactions:

1. $(BR_2H)_2$ → 2 BR_2H
2. $(BR_2H)_2$ + 2 S → 2 S-BR_2H
3. $(BR_2H)_2$ + S → S-BR_2H + BR_2H
4. S-BR_2H → S + BR_2H
5. BR_2H + substrate → product
6. S-BR_2H + substrate → S + product

Here S is a nucleophilic solvent molecule (ether, amine, etc.) that forms a Lewis acid/base adduct with a borane, e.g. a B-O bond to ethers. Brown felt that dissociation of the borane dimer (step 1) was only important for non-nucleophilic solvents, i.e. that nucleophilic ethers replace step 1 by steps 3 and 4 with an adduct intermediate, causing a lowering of the overall activation energy and hence a faster reaction rate. Since the monomer BR_2H was not present in appreciable amounts, step 2 was the equilibrium monitored in the experiments. He also felt that the actual hydroboration step is 5, rather than 6, although this was challenged by Schleyer and recently only cautiously supported by Singleton.

We considered tetrahydrofuran (THF, C_4H_8O) as the solvent S, isobutene (C_4H_8) as the substrate, and two different choices for the borane BR_2H: 9-BBN (9-borabicyclo[3.3.1]nonane, $C_8H_{15}B$) and the simple borane BH_3. We examined Brown's infrared and ^{11}B-NMR arguments, his equilibrium constant for reaction 2, and performed transition-state searches.

2. COMPUTATIONAL DETAILS

Geometry optimizations were performed with Gaussian03 using various density-functional theory (DFT) methods: B3LYP, PBEPBE, and OLYP. Basis sets employed were 6-31G(d), 6-31G(d,p), and cc-pVDZ. For GIAO NMR calculations, B3LYP/6-311+G(d,p) was employed. For energetics, single-point energies were computed with the coupled-cluster approximation CCSD(T)/cc-pVDZ//B3LYP/6-31G(d) using MOLPRO2008.

Conformer studies were performed on 9-BBN, (9-BBN)$_2$, and THF (**Table 2.1**). The lowest-energy forms of 9-BBN and its dimer (dd and dd:dd, see **Fig. 2.1**) were used in ensuing computations. The choice of conformer for THF is a tricky problem because of the low-frequency pseudorotation mode, which connects many structures of different symmetry (C_1, C_2, C_s) having nearly equal energy. Different levels of theory disagree on which symmetry form is the global minimum. We found it simplest to choose C_s symmetry for THF and its borane adducts, for this made the pseudorotation mode have an imaginary frequency for B3LYP calculations; this was desired because it removes the overly large entropy estimation of the low frequency mode (due to error in the harmonic approximation) from entropy computation.

Table 2.1. Relative energies of conformers, B3LYP/6-31G(d).

Molecule	Conformer	Energy (kJ/mol)
9-BBN	dd	0
	du	1.2
	uu	33.8
(9-BBN)$_2$	dd:dd	0
	ud:dd	7.2
	ud:uu	13.8
	ud:du	14.3
THF	C1	0.4
	C2	0
	Cs	0.4
	C2v	13.9

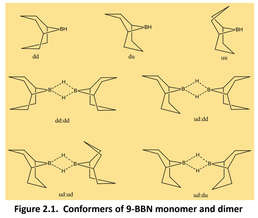

Figure 2.1. Conformers of 9-BBN monomer and dimer

3. RESULTS & DISCUSSION

3.1 SPECTRAL SIGNATURES

Infrared spectra were used by Wang and Brown[1] to identify the presence of the 9-BBN-THF adduct. In the B-H stretch region, they attributed a small peak at 2300 cm^{-1} to be due to the adduct, and a strong peak at 1570 cm^{-1} to be due to BH bridge bonds of the (9-BBN)$_2$ dimer. By converting our computed harmonic frequencies **ω** to fundamentals **ν** using a recommended scaling factor of 0.9875[6] we obtain computed values only 2% larger than the experimental values (a scaling factor of 0.965 would have been ideal), thus supporting the experimental assignment (**Table 3.1.1**). The corresponding absorption for a monomer would be near 2460-2520 cm^{-1}, which was apparently not observed. The relevant PBEPBE predicted spectra appear in **Fig. 3.1.1**.

The ^{11}B-NMR spectrum was also used by Wang and Brown[1] to identify the presence of the 9-BBN-THF adduct. They attributed observed signals to the (9-BBN)$_2$ dimer and 9-BBN-THF complex, which we confirm with B3LYP calculations presented in **Table 3.1.2**.

Table 3.1.1. The signature BH stretch infrared mode, PBEPBE/6-31G(d)

Species	DFT ω, cm^{-1}	DFT [a] ν, cm^{-1}	Expt [b] ν, cm^{-1}
9-BBN	2551	2519	n/a
THF-9-BBN	2377	2347	2300
(9-BBN)$_2$	1632	1612	1570

[a] Using 0.9875 scale factor.[6]

[b] Wang and Brown.[1]

Table 3.1.2. ^{11}B{^{1}H}-NMR chemical shifts, GIAO B3LYP/6-311+G(d,p)//B3LYP/6-31G(d).

Species	DFT δ absolute	DFT δ relative	Expt [a] δ relative
BF_3-OEt_2	101.5	0	0
9BBN-THF	83.9	17.6	13.8
(9BBN)$_2$	75.3	26.2	27.7
9BBN	8.5	93	n/a

[a] Wang and Brown.[1]

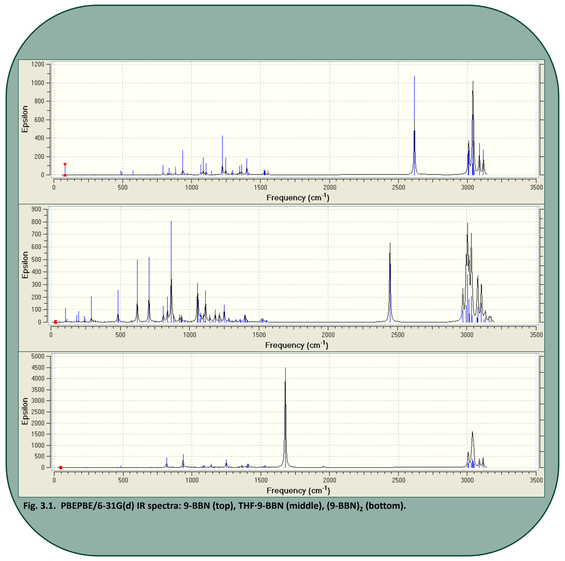

Fig. 3.1. PBEPBE/6-31G(d) IR spectra: 9-BBN (top), THF-9-BBN (middle), (9-BBN)$_2$ (bottom).

3.2. ENERGIES

Reaction energies and equilibrium constants for the six reactions are reported in **Table 3.2.1**. The results obtained using B3LYP are in close agreement with CCSD(T), where the larger basis set gave the closest results and reaction energies for BH_3 are closer than for 9-BBN. Reaction energies obtained via OLYP where much worse than B3LYP and PBEPBE, however BH_3 was much better than 9-BBN. PBEPBE gave reaction energies further from CCSD(T) than B3LYP, but much better than OLYP. With respect to all levels of theory, reaction energies for reaction 6 were in close agreement while the energies for reaction 2, and to a lesser extent reaction 4, are very far from CCSD(T).

Table 3.2.1. Comparison of reaction energies in kJ/mol.

Reaction	Species	AM1	B3LYP cc-pVDZ	B3LYP 6-311G(d,p)	B3LYP 6-31G(d)	OLYP 6-31G(d)	PBEPBE 6-31G(d)	CCSD(T) cc-pVDZ
1	BH_3	129.1	165.5	168.4	163.5	174.9	213.4	164.9
	9BBN	31.3	104	102.4	97.9	99.4	144.4	153.7
4	BH_3	88.1	89	88.3	88.1	67.3	107.1	98.7
	9BBN	15.9	46.9	45.5	45	12.1	62.3	92.6
2	BH_3	-47.1	-12.6	-8.2	-12.7	40.4	-0.8	-32.6
	9BBN	-0.6	10.1	11.4	7.9	75.1	19.8	-31.6
5	BH_3	-198.6	-108.5	-109.6	-107.6	-98.8	-135.5	-118.6
	9BBN	-174.1	-98.8	-100.2	-98.6	-86.8	-118.8	-128.4
6	BH_3	-110.4	-19.5	-21.3	-19.4	-31.5	-28.4	-19.9
	9BBN	-158.2	-51.8	-54.7	-53.6	-74.7	-56.5	-35.8
1	Keq $(BH3)_2$	2.40E-23	1.00E-29	3.20E-30	2.20E-29	2.30E-31	4.00E-38	1.30E-29
	Keq $(9BBN)_2$	3.30E-06	6.10E-19	1.20E-18	7.00E-18	3.90E-18	5.00E-26	1.20E-27
4	Keq THF.BH_3	3.60E-16	2.50E-16	3.40E-16	3.60E-16	1.60E-12	1.70E-19	5.00E-18
	Keq THF.9BBN	1.60E-03	6.00E-09	1.10E-08	1.30E-08	7.50E-03	1.20E-11	5.90E-17
2	Keq (BH_3)	1.80E+08	1.60E+02	2.70E+01	1.70E+02	8.50E-08	1.40E+00	5.00E+05
	Keq (9BBN)	1.30E+00	1.70E-02	1.00E-02	4.20E-02	7.00E-14	3.40E-04	3.40E+05

3.3 MEASURABLE EQUILIBRIUM

Brown was able to measure the equilibrium constant of reaction 2 using (9-BBN)$_2$, for which he reported K = 8.05 × 10^{-5} M^{-1}. The accuracy of our computations can be gauged by comparing our computed thermodynamic equilibrium constants for reaction 2 via:

$$K^{\Delta G} = K^{conc} \cdot [THF] = (8.05 \times 10^{-5}\ M^{-1}) \cdot (12.3\ M) = 1.0 \times 10^{-3}$$

By inspection of **Table 3.3.1** it appears that the equilibrium constant for reaction 2 calculated from the gas-phase free energies are far smaller than the experimental value, and may be due to the fact that gas-phase entropies are larger than in solution. Since the equilibrium constants calculated from free energies may be questionable, equilibrium constants calculated from electronic energies and enthalpies may be considered. Excluding the OLYP results, the equilibrium constants calculated from electronic energies and enthalpies give values are comparable to Brown.

Table 3.3.1. Computed equilibrium constants for reaction 2.

Method	ΔE, (kJ/mol)	ΔH, (kJ/mol)	ΔG, (kJ/mol)	K from ΔE	K from ΔH	K from ΔG
PBEPBE/6-31G(d)	19.8	0.7	83.0	3.4E-04	7.7E-01	2.8E-15
B3LYP/6-31G(d)	7.9	12.6	60.3	4.2E-02	6.3E-03	2.7E-11
B3LYP/6-31G(d,p)	11.4	16.0	63.9	1.0E-02	1.6E-03	6.3E-12
OLYP/6-31G(d)	75.1	79.8	125.2	7.0E-14	1.0E-14	1.2E-22
B3LYP/cc-pVDZ	10.1	9.0	70.0	1.7E-02	2.6E-02	5.5E-13

3.4 THE FULL PATHWAY

The reaction pathway for the hydroboration of isobutene is depicted in **Figure 3.4.1**. **Figure 3.4.2** shows the general potential energy surface (PES) for the reaction pathway of the hydroboration of isobutene with B_2H_6 in THF solvent. Considering the interactions of reactants prior to the reaction, and the interactions of the formed products, the full PES is depicted in **Figure 3.4.3**. Note that the largest activation energy on the full path, 56 kJ/mol, is far less than the 165 kJ/mol required to dissociate B_2H_6 on the uncatalyzed pathway. The analogous TS-2 and TS-3 shown in **Figure 3.4.1** for borane are not believed to exist for 9-BBN do to steric constraints.

The full PES shown in **Figure 3.4.3** contains additional data points for TS-1 reactants 1, TS-1 products 1, TS-2 reactants 1, TS-2 reactants 2, TS-2 products 1, TS-3 reactants 1, TS-3 products 1, TS-3 products 2. Interactions leading to these points are displayed in **Figure 3.4.4**, except for TS-2 Reactants 2 datum point, which represents an energy shelf in the optimization of TS-2 reactants 1.

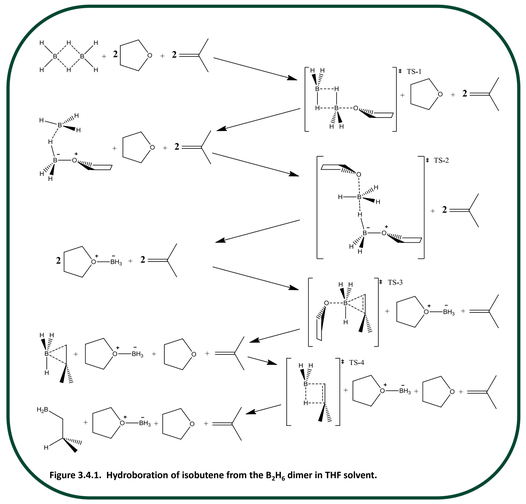

Figure 3.4.1. Hydroboration of isobutene from the B_2H_6 dimer in THF solvent.

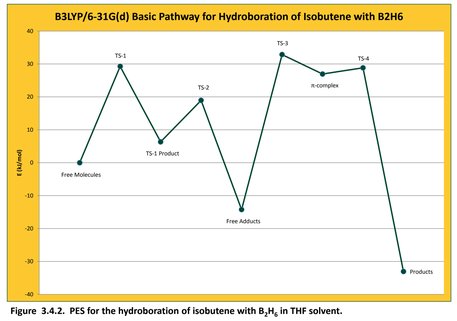

Figure 3.4.2. PES for the hydroboration of isobutene with B_2H_6 in THF solvent.

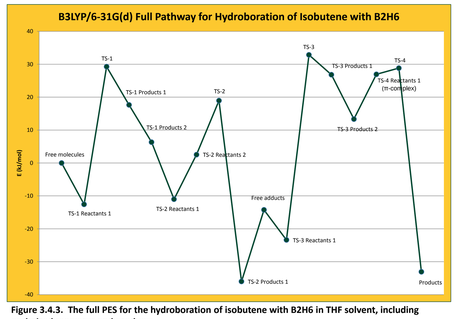

Figure 3.4.3. The full PES for the hydroboration of isobutene with B2H6 in THF solvent, including optimized reactants and products.

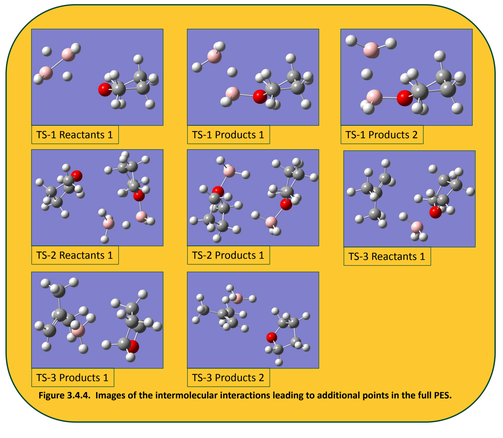

Figure 3.4.4. Images of the intermolecular interactions leading to additional points in the full PES.

3.5 THE PREDOMINATING MECHANISM

Considering the proposed catalytic mechanism of Brown,[1] it is illustrated in **Table 3.5.1** that substituting reactions 3 and 4 for 1 results in two lower reaction energy barriers. With respect to attack of the alkene, Reaction 5 on the PES in **Figures 3.4.2** and **Figure 3.4.3** is found to be 98 kJ/mol, almost double the activation energy for reaction 6 (56 kJ/mol). Therefore it is likely that alkene attack by the borane-THF complex as suggested by Schleyer[2] is the predominating mechanism.

Table 3.5.1. B3LYP/6-31G(d) activation energies displaying catalytic effects of THF solvent.

Borane Species	Reaction	Ea (au)	Ea (kJ/mol)
BH_3	1	0.0623	163.54
	3	0.0111	29.26
	4	0.0339	88.89
9-BBN	1	0.0373	97.91
	3	0.0303	79.44
	4	0.0170	44.61

4. CONCLUSION

- ✓ The data resulting from investigation into the spectral signatures reported by Brown has proved that IR and NMR can be used to detect reaction intermediates.
- ✓ It is likely that Schleyer's suggestion for the last step, reaction 6, is predominating over reaction 5 in the case of B_2H_6.
- ✓ An ether solvent such as THF results in lower reaction barriers relative to the dissociation of borane dimers in a non ether type solvent, which explains the observed catalytic effect.

ACKNOWLEDGEMENTS

- Colin M. Kuntz.
- Rachelle A. Mondor.
- John G. Ottaviano.
- Arumugam Jayaraman.
- Aravind V. Rayer†.
- NSERC.
- Gaussian Inc.
- MOLRPO developers H.-J. Werner and P. J. Knowles.
- CFI for the purchase of entropy, a 2010 Ciaratech FUSSION SMP supercomputer (shared memory) and dextrose, a 2010 Ciaratech supercomputer cluster (distributed memory).
- Laboratory for Computational Discovery, Department of Science, University of Regina (John Jorgensen, sysadmin).
- Department of Computer Science for use of facilities in Chemistry 461.

† Department of Industrial Systems Engineering, University of Regina.

REFERENCES

[1] Wang, K. K.; Brown, H. C. *J. Am. Chem. Soc.* **1982**, *104*, 7148.
[2] Clark, T.; Wilhelm, D.; Schleyer, P. v. R. *J. Chem. Soc., Chem. Commun.* **1983**, 606.
[3] Wang, X.; Li, Y.; Wu, Y.-D.; Paddon-Row, M. N.; Rondan, N. G.; Houk, K. N. *J. Org. Chem.* **1990**, *55*, 2601.
[4] Ess, D. H.; Kister, J.; Chen, M.; Roush, W. R. *J. Org. Chem.* **2009**, *74*, 8626.
[5] Oyola, Y.; Singleton, D. A. *J. Am. Chem. Soc.* **2009**, *131*, 3130.
[6] J. P. Merrick, D. Moran, and L. Radom, J. Phys. Chem. A 2007, 111, 11683.

CHEMISTRY RESEARCH AT THE U of R

Dr. Allan East's research interests are in the development and application of theoretical/computational methods to explore the structures, strengths, and effects of weak bonds in chemistry. One set of applications is in understanding catalytic mechanisms of petroleum refining, while another is thestudy of excited (excimer) states of weakly bound complexes such as benzene dimer. Transition-state optimization and ab initio molecular dynamics (AIMD) simulations are performed with a 420-processor supercomputer.

Dr. Lynn Mihichuk's research interests include a study of seven coordinate tungsten complexes, including synthesis, X-ray structural studies, NMR studies (1H, 13C, 31P, 183W) and computational studies. In addition, he is pursuing catalytic applications of seven coordinate tungsten complexes in the ring opening metathesis polymerization reactions.

Recent studies in **Dr. Scott Murphy's** research program have focused on the synthesis and incorporation of photochromic compounds into the lipid bilayer of a liposome as a strategy for controlling membrane permeability with the use of light. Photochromes of interest belong to the dithienylethene and spirooxazine families. The resulting photochromic liposomes are currently being developed for their potential applications in photoregulated liposomal drug delivery.

Dr. Renata Raina's research interests include (a) studies on the atmospheric transport and transformation of pesticides in soil and air and (b) the analysis of lead and other trace metals in groundwater. Present research includes examining the feasibility of filtration in lead analysis of groundwater samples containing colloidal material and sediments; and studies of the variability of trace metals and pesticides in soil and air samples from forested and agricultural sites. Research efforts also include examining processes of transformation of pesticides including development of chromatographic methods.

Research in **Dr. Brian Sterenberg's** group is focused on inducing unusual reactivity by using transition metal complexes to put atoms into unusual environments. We have two main research areas: the transition metal chemistry of phosphorus and metal templated synthesis. Transition metal coodination can be used to stabilize reactive phosphorus groups such as phosphido (PR2-) and phosphinidene (PR). These metal-coordinated fragments show unique reactivity, including bond insertion reactions and cycloadditions, which have potential applications to organophosphorus sythesis. Metal templated synthesis is the use of metal coordination to pre-arrange reactive substrates. We use metal templation to control alkyne cycloaddition reactions, and apply this methodology to the contruction of novel ring systems.

Dr. Andrew Wee's research interests include (a) The development of Rh(II) carbenoid based methodologies for heterocyclic synthesis and (b) The synthesis and use of chiral, nonracemic heterocyclic building blocks in the synthesis of natural products, in particular alkaloids. Present efforts are aimed at the total synthesis of indole alkaloids such as quebrachamine, eburnamonine as well as piperidine alkaloidstypified by pseudodistomins A and B, and the prosopis family of alkaloids.